



HAL
open science

Niche breadth of Amazonian trees increases with niche optimum across broad edaphic gradients

Jason Vleminckx, Oscar Valverde Barrantes, Claire Fortunel, C. E. Timothy Paine, David Bauman, Julien Engel, Pascal Petronelli, Nállarett Dávila, Marcos Rios, Elvis Harry Valderrama Sandoval, et al.

► To cite this version:

Jason Vleminckx, Oscar Valverde Barrantes, Claire Fortunel, C. E. Timothy Paine, David Bauman, et al.. Niche breadth of Amazonian trees increases with niche optimum across broad edaphic gradients. *Ecology*, 2023, 104 (7), pp.e4053. 10.1002/ecy.4053 . hal-04098939

HAL Id: hal-04098939

<https://hal.inrae.fr/hal-04098939>

Submitted on 26 Oct 2023

HAL is a multi-disciplinary open access archive for the deposit and dissemination of scientific research documents, whether they are published or not. The documents may come from teaching and research institutions in France or abroad, or from public or private research centers.

L'archive ouverte pluridisciplinaire **HAL**, est destinée au dépôt et à la diffusion de documents scientifiques de niveau recherche, publiés ou non, émanant des établissements d'enseignement et de recherche français ou étrangers, des laboratoires publics ou privés.

1 1. Title page

2 **Journal name:** *Ecology*

3 **Manuscript type:** *Article*

4 **Title:**

5 Niche breadth of Amazonian trees increases with niche optimum across broad edaphic
6 gradients.

7 **Author list and affiliation**

8 Jason Vleminckx^{1,2,3}, Oscar Valverde Barrantes^{2,4}, Claire Fortunel⁵, C.E. Timothy Paine⁶,
9 David Bauman^{5,7}, Julien Engel^{4,5}, Pascal Petronelli⁸, Nállarett Dávila^{9†}, Marcos Rios⁹, Elvis
10 Harry Valderrama Sandoval¹⁰, Italo Mesones¹¹, Elodie Allié^{8,12}, Jean-Yves Goret¹², Freddie C.
11 Draper¹³, Juan Ernesto Guevara Andino¹⁴, Solène Bérroujon¹⁵, Paul V. A. Fine¹⁶, Christopher
12 Baraloto^{2,4,12}

13

14 1. Yale Institute For Biospheric Studies (YIBS), Yale University, New Haven, CT, USA.

15 ORCID: 0000-0001-7557-0866.

16 2. Department of Biological Sciences and Institute of Environment, Florida International Univ.,

17 FL, USA.

18 3. Plant Ecology and Biogeochemistry lab, Faculty of Sciences, Université Libre de Bruxelles,

19 Brussels, Belgium.

20 4. International Center for Tropical Botany, Dept of Biological Sciences, Florida International

21 Univ., Miami, FL, USA.

22 5. AMAP (Botanique et Modélisation de l'Architecture des Plantes et des Végétations),

23 Université de Montpellier, CIRAD, CNRS, INRAE, IRD, Montpellier, France.

24 6. Environmental and Rural Science, Univ. of New England, Armidale, New South Wales,

25 Australia.

† This author is deceased

- 26 7. Environmental Change Institute, School of Geography and the Environment, University of
27 Oxford, Oxford, UK.
- 28 8. CIRAD, UMR Ecologie des Forêts de Guyane, AgroParisTech, Univ. De Guyane, Univ. Des
29 Antilles, Kourou Cedex, France.
- 30 9. Instituto de Investigaciones de la Amazonia Peruana, Iquitos, Peru, Avenida José A.
31 Quiñones km 2.5, Iquitos, Loreto Perú.
- 32 10. Facultad de Ciencias Biológicas, Universidad Nacional de la Amazonía Peruana, Iquitos,
33 Loreto, Perú.
- 34 11. Department of Integrative Biology and University and Jepson Herbaria, University of
35 California, Berkeley, 3040 Valley Life Sciences Building 3140, Berkeley, California
36 94720-3140 USA.
- 37 12. INRAe, UMR Ecologie de Forêts de Guyane, AgroParisTech, CIRAD, INRA, Univ. de
38 Guyane, Univ. des Antilles, Kourou Cedex, France.
- 39 13. Center for Global Discovery and Conservation Science, Arizona State University, 1001
40 South McAllister Avenue Tempe, Tempe, Arizona 85287 USA.
- 41 14. Field Museum of Natural History, Chicago, IL, USA. ORCID: 0000-0002-5433-6218.
- 42 15. EcoFoG, UMR Ecologie des Forêts de Guyane, AgroParisTech, Univ. de Guyane, Univ.
43 des Antilles, Kourou Cedex, France.
- 44 **Corresponding author:** Jason Vleminckx (email: jasv1x86@gmail.com).
- 45 **Open Data Agreement:** Data is available in Vleminckx et al. (2023), provided through the
46 Harvard Dataverse repository: <https://doi.org/10.7910/DVN/VWAJYR>
- 47 **Key-words:** abiotic filtering, competitive exclusion, functional traits, Neotropical forests,
48 niche breadth, niche position, range of resource use, soil nutrient availability, tree community
49 assembly.

50 2. Abstract

51 Understanding how biotic interactions and environmental filtering mediated by soil
52 properties shape plant community assembly is a major challenge in ecology, especially when
53 studying complex and hyper-diverse ecosystems like tropical forests. To shed light on the
54 influence of both factors, we examined how the edaphic optimum of species (their niche
55 position) relates to their edaphic range (their niche breadth) along different environmental
56 gradients, and how this translates into functional strategies.

57 Here we test four scenarios describing the shape of the niche breadth – niche position
58 relationship, including one neutral scenario and three scenarios proposing different relative
59 influences of abiotic and biotic factors on community assembly along a soil resource gradient.
60 To do so, we used soil concentration data for five key nutrients (N, P, Ca, Mg and K), along
61 with accurate measurements of 14 leaf, stem and root traits for 246 tree species inventoried in
62 101 plots located across Eastern (French Guiana) and Western (Peru) Amazonia.

63 We found that species niche breadth increased linearly with species niche position along
64 each soil nutrient gradient. This increase was associated with more resource acquisitive traits
65 in the leaves and the roots for soil N, Ca, Mg and K concentration, while it was negatively
66 associated with wood density for soil P concentration. These observations agreed with one of
67 our hypothetical scenarios in which species with resource conservation traits are confined to
68 the most nutrient-depleted soils (abiotic filter), but they are outperformed by faster-growing
69 species on more fertile conditions (biotic filter). Our results refine and strengthen support for
70 niche theories of species assembly, while providing an integrated approach to improve forest
71 management policies.

72 3. Main text

73 **Introduction**

74 A major interest among plant community and evolutionary biologists is to better
75 understand how environmental filtering and biotic interactions shape community assembly.
76 Many studies examining the determinants of plant β -diversity have emphasized the role of
77 abiotic conditions, such as soil properties, through filtering processes related to species resource
78 acquisition strategies and tolerance to drought and toxicity (Condit et al. 2013, Kraft et al. 2015,
79 Vleminckx et al. 2017, Van Breugel et al. 2019). Several theories have suggested that
80 hyperdiverse communities such as tropical forests also experience strong biotic interactions,
81 mediated by intense inter-specific competition for resources and enemy attacks (Schemske
82 2009, Fine 2006, 2013). Over time, these biotic interactions would have resulted in the local
83 coexistence of species displaying narrower species niches (Dobzhansky 1950, Pianka 1966,
84 MacArthur 1969).

85 Habitat heterogeneity remains a major determinant of species turn-over in tropical
86 forests. In the Amazon, for instance, white-sand habitats show extremely nutrient-depleted
87 conditions that select for species investing into costly but well-defended tissues (e.g. thick
88 leaves, hard wood), which render these species less competitive on relatively more fertile
89 conditions (the growth-defense trade-off; Fine et al. 2006, 2010). Species relative investment
90 in costly tissues should therefore reflect their optimum along a resource availability gradient.
91 This optimum should correlate well with the range of resource availability a species can
92 tolerate, under the assumption that poor-soil specialists are poor competitors in fertile
93 conditions and are thereby confined to more restricted niches than faster-growing, rich-soil
94 specialists. Therefore, comparing the range and optimum of species along a steep resource
95 availability gradient would help to determine whether conservative species with a high degree
96 of specialization for poor soil conditions exhibit narrower niches than acquisitive species that

97 grow faster and are more competitive in fertile soils (assuming that no other processes are
98 becoming important across a broad gradient in soil fertility). Such a comparison would address
99 a major concern that most studies may overstate the role of abiotic filtering as a community
100 assembly rule because they fail to consider the potential influence of biotic processes ([Kraft et
101 al. 2014](#)). Additionally, examining how species range and optimum align with different
102 functional strategies may help to identify adaptive trade-offs that delimit species' niches.
103 Despite the rapid accumulation of plant functional trait data from diverse ecosystems, few
104 studies have attempted to link tree species range, optimum, and functional traits (but see
105 [Treurnicht et al. \[2019\]](#) for Fynbos plant communities of the Cape Floristic Region).

106 Species niche range and optimum relate to the two fundamental parameters proposed by
107 Hutchinson in his hypervolume model ([1957](#)), which has provided one of the most successful
108 mechanistic constructs of the ecological niche concept. The niche range is commonly referred
109 to as “niche breadth”, “niche width”, “niche size”, or “ecological amplitude” ([Carscadden et al.
110 2020](#)). Following the Hutchinson’s concept of the niche, the niche breadth determines the range
111 of environmental conditions that a species can tolerate and the range of resources that it uses
112 (the potential, or fundamental niche), a range that in reality is more contracted due to
113 antagonistic interactions mediated by competition for resources, natural enemies, or dispersal
114 barriers (the realized, or observed niche) ([Malanson, Westman & Yan 1992](#); [McGill et al. 2006](#);
115 [Kraft et al. 2014](#)). The niche optimum represents the set of environmental conditions where the
116 fitness of a species is highest, as reflected by growth rate, reproduction success, survival,
117 population size or distribution range ([Sexton et al. 2017](#)). This parameter can be assessed by
118 calculating the niche position, which can be defined as the average, or median value of an
119 environmental variable where the species occurs, or sometimes as the marginality of this
120 average value compared to the community mean ([Roughgarden 1974](#)). The niche position is
121 generally used as a proxy for the niche optimum, since the “true” optimal conditions for a

122 species is generally unknown (as its “true” niche breadth) or only estimated via habitat
123 suitability models (Zuquim et al. 2019). Most studies examine species distributions across only
124 a portion of their geographic and environmental ranges (Sheth et al. 2020), with sampling
125 protocols that are rarely explicitly designed to cover an exhaustive representation of the habitat
126 heterogeneity occurring within a study area, or to provide an equilibrated sampling effort across
127 contrasted habitat conditions.

128 We can propose at least four hypothetical scenarios predicting the shape of niche
129 breadth-position relationships along a gradient of soil nutrient availability (Fig. 1). The
130 relationship between realized species niche breadth and niche position, as well as with their
131 traits, can be illustrated using Gaussian-like curves for simplicity, as in the classic resource
132 utilization model of McArthur (1958) (Fig. 1a), even though actual distributions may follow
133 other forms (Le Bagousse-Pinguet et al. 2017). These curves can be translated into values
134 describing the relationship of niche breadth plotted against niche position (Fig. 1b).

135 In the first scenario, species niche breadth varies randomly across species, regardless of
136 their niche position along a gradient of soil resource availability. This pattern would arise if
137 species were competitively equivalent on any level of that specific soil resource availability,
138 i.e. if species edaphic distribution is only driven by stochastic and dispersal processes. In that
139 sense, this scenario is consistent in its outcome with Hubbell’s neutral theory (2001). In the
140 second scenario, poor soil resources select for species investing in protection against physical
141 and biological damages, to the detriment of growth, which would render these species
142 increasingly less competitive when soil fertility increases. In this case, niche breadth should
143 increase with niche position, and the strength (slope) of this relationship should reflect how
144 much the cost of adaptation to nutrient-poor soils restricts the ability of conservative species to
145 compete with more acquisitive species and establish in more fertile habitats. This scenario is
146 consistent with previous studies showing that poor-soil specialists exhibit resource conservation

147 strategies (e.g. durable tissues with slow turnover), whereas species preferring more fertile soils
148 are characterized by resource acquisitive traits (e.g. cheap tissues with high turnover) (Fine et
149 al. 2006, Pinho et al. 2017, Poorter et al. 2018). Scenario 3 is similar to the second scenario,
150 except that the soil nutrient is not limiting for any species beyond a certain threshold, above
151 which the nutrient availability does not impact fitness anymore. Niche breadth therefore tends
152 to reach a plateau. Such a pattern has rarely been emphasized but see Steidinger (2015) for soil
153 calcium concentration optimum in Panama, which stabilizes and shows a trend consistent with
154 scenario 3. In the fourth scenario, the increase of potential niche breadth as soil resource
155 availability becomes less limiting is counter-balanced by a greater “species packing”, i.e. a
156 constriction of species’ realized niches (MacArthur 1969) resulting from stronger competition
157 for resources. In this scenario, niche breadth increases with soil resource availability optima,
158 up to a certain intermediate level of soil fertility, then decreases as a consequence of species
159 packing, forming a bell-shaped curve.

160 To further shed light on the goodness-of-fit of each scenario to real species assemblages,
161 we may also inquire whether niche breadth-position relationships show consistent patterns
162 along decoupled environmental gradients, and whether the same functional trade-offs align
163 along each gradient. Environmental axes may covary, or vary independently from each other,
164 either because they are spatially structured at different spatial scales (e.g. climate vs
165 microhabitat variables), or in the case of soil properties because they are influenced by different
166 pedological or biogeochemical processes. For instance, some key soil nutrients like base cation
167 (e.g. calcium, magnesium, potassium) are known to covary, as their concentrations depend on
168 common chemical and geological conditions (e.g. soil acidity, nature of the bedrock). Other
169 soil variables, notably anionic nutrients (e.g. PO_4^{3-} , NO_3^{2-}), may display decoupled spatial
170 variations, as they undergo different chemical constraints (e.g. P immobilization) or different
171 biogeochemical processes (e.g. N-fixation, nitrification) (Hedin et al. 2009, Vleminckx et al.

172 [2015, Quesada et al. 2010](#)). Whether we observe similar niche breadth-position relationships
173 along decoupled environmental dimensions, or whether niche breadth and niche position are
174 influenced by the same resource use traits along those environmental dimensions, are key
175 questions to improve our understanding of community assembly mechanisms. However, these
176 questions remain poorly examined ([Futuyma and Moreno 1988, Sultan et al. 1998, Carscadden
177 et al. 2020](#)).

178 The “world-wide plant economics spectrum hypothesis” ([Reich 2014](#)) suggests that fast-
179 slow economics spectra would be consistently observed along decoupled soil fertility gradients,
180 with resource conservation traits being selected on nutrient-depleted soils in general. Although
181 some evidence has supported this hypothesis ([Poorter et al. 2018](#)), previous studies have also
182 shown that tree communities display decoupled trait syndromes across leaf, stem and roots
183 ([Baraloto et al. 2010, Fortunel et al. 2012, Laughlin 2014, Vleminckx et al. 2021, Asefa et al.
184 2022](#)). These decoupled wood and leaf economic traits have been shown to respond to similar
185 fertility gradients in tropical forests ([Fortunel et al 2014, Vleminckx et al. 2021](#)). Yet, to date
186 there has been no attempt to integrate niche breadth data to examine how individual nutrient
187 availability gradients potentially determine species edaphic ranges, and whether decoupled
188 traits align with the same fertility gradients.

189 Here, we address these questions using a unique dataset of 246 tree species inventoried
190 in 101 plots located across Eastern (French Guiana) and Western (Peru) Amazonia, together
191 with accurate measurements of 14 leaf, stem and root traits. We first examine whether species
192 niche breadth and niche position, taken separately, are aligned or decoupled among five soil
193 nutrient availability gradients (N, P, Ca, Mg and K). Second, we examine how well the four
194 scenarios presented in Fig. 1 match the observed niche breadth-position relationship along each
195 soil gradient. We address the following specific questions:

- 196 (1) How are species niche breadth and position associated among the different soil
197 nutrient gradients?
- 198 (2) How well do our four scenarios (Fig. 1) fit the niche breadth-position relationship?
- 199 (3) Are decoupled niche breadth and position dimensions associated with different plant
200 functional strategies?

201 **Methods**

202 **Study areas**

203 We established a nested experimental design with replicated plots in habitats displaying
204 contrasting soil conditions, characteristic of lowland Amazonian forests – white-sand (WS),
205 Terra Firme (TF) and seasonally flooded forests (SF) (Fortunel et al. 2014, Baraloto et al. 2021)
206 – at both regional (c.100 km) and basin-wide (2500 km) distances. A total of 101 0.1-ha plots
207 were inventoried between 2008 and 2018 in ten subregions of tropical moist forest in French
208 Guiana (hereafter FG; 63 plots) and between 2008 and 2011 in three subregions in Peru (38
209 plots) (Fig. 2). French Guiana forests stand on an old Precambrian tableland, with old, highly
210 weathered and nutrient-depleted soils (Gourlet-Fleury et al. 2004). Mean annual rainfall across
211 inventory subregions ranges between 2160 and 3130 mm (<http://www.worldclim.com/>) and is
212 distributed seasonally throughout the year. The wet season stretches from December to July and
213 is usually interrupted in February or March by a short dry period, while the dry season occurs
214 from August to November with monthly rainfall never exceeding 100 mm. Mean temperature
215 oscillates between 23.0 and 26.6°C with low seasonal variation (Gourlet-Fleury et al. 2004).
216 Elevation among subregions ranged from 42 to 529 m. Forests from the Western Amazon in
217 Peru cover heterogeneous soil conditions consequent to the combined impact of marine
218 incursions, the Andean uplift, and the weathering of volcanic sediments (Hoorn et al. 2010).
219 Mean annual rainfall varies between 2405 and 2750 mm, whereas mean temperature ranges

220 from 26.3°C to 26.7°C (<http://www.worldclim.com/>), and elevation from 95 to 173 m. The
221 study areas are further detailed in Baraloto et al. (2021).

222 **Tree species inventories**

223 Trees were inventoried following a modified version of the Gentry plots proposed by Phillips
224 et al. (2003) and described by Baraloto et al. (2013). Each plot consisted of ten parallel 50 m-
225 long transects departing perpendicularly from a main 180 m-long central line, successively in
226 alternate directions every 20 m along the line (a schematic illustration of a plot is provided in
227 Appendix S1: Figure S1). All stems with a circumference ≥ 8 cm at 1.3 m above the ground
228 (2.5 cm DBH) were inventoried over a two-meter width along each transect. At least one
229 individual of every putatively-distinct taxon encountered was collected in the field to create
230 plot-level voucher collections. In rare cases (0.2% of all stems sampled), no identification was
231 achieved nor could vouchers be collected due to lack of leaves or obstructed canopies. The plot
232 level vouchers were meticulously sorted so that independent distinct taxa had at least one
233 collection in each plot. Further sorting resulted in standardized project type collections for all
234 distinct taxa which were identified at regional herbaria for the Peru (AMAZ) and French Guiana
235 (CAY) collections. We then further standardized and resolved vouchers from both these
236 collections during a five-month period at the herbarium of the Missouri Botanical Garden (MO),
237 such that any unnamed, putative novel species was compared to other congeners from the other
238 region (Baraloto et al. 2021). At the end, we provided a full detail of all project vouchers
239 describing our standardized inventories (vouchers and/or photos are available for loan upon
240 request). Species diversity was characterized in each subregion using species richness, as well
241 as the effective number of species expected from 1000 random samplings of 2 individuals to
242 weight for species abundance (Dauby & Hardy 2011) (Table 1).

243 **Soil data**

244 We collected bulked soil cores at 0–15 cm depth at ten regularly spaced positions along the
245 central line of the plot (Appendix S1: Figure S1). The ten cores were mixed into a 500 g sample
246 that was dried to constant mass (at 25°C) and sieved (2 mm mesh). Samples from were shipped
247 to the University of California, Davis DANR laboratory for physical and chemical analyses (see
248 [Baraloto et al. 2011](#) for full protocol details). The bioavailability of three base cations (Ca, Mg,
249 K) and P, and the total soil nitrogen concentration (N) were then quantified for each soil sample,
250 following a protocol described in details Baraloto et al. (2011). We lack data on other soil
251 variables like soil pH and soil Al, Mn and Fe concentration to evaluate the impact of soil acidity
252 and toxicity on species niches. The mean and the standard deviation of each soil variable in
253 each habitat and each study region (Peru and French Guiana, separately) is shown in Table 2.
254 The distribution of plot values for each soil variable within each edaphic habitat (SF, TF and
255 WS), and a test of comparison (Wilcoxon-Mann-Whitney) of these values across habitats for
256 each soil variable are shown in supplementary information (Appendix S2: Figure S1). As a
257 complementary information, we also show the projection of plots and soil variables in a
258 Principal Component Analysis (PCA) (see details in Appendix S3: Figure S1).

259 **Functional trait data**

260 We used data for 14 chemical and morphological traits related to resource use and structural
261 defense, comprising ten leaf, two stem and two fine root traits: Leaf thickness and toughness,
262 SLA, Leaf C, N, P, Ca, Mg and K concentration, leaf ¹³C, sapwood-specific gravity, trunk bark
263 thickness, fine root tissue density and fine root specific root length (SRL). The unit and
264 functional role of each trait, along with additional information on trait sampling locations are
265 provided as online supplementary information ([Vleminckx et al. 2023](#)). These functional data
266 were obtained from accurate trait measurements from Peruvian and French Guianan samples
267 collected for 8345 individuals from 1625 species in 371 genera, 78 families and 26 orders

268 covering the Rosidae, Asteridae and early eudicots (Baraloto et al. 2010, Fortunel et al. 2012,
269 Vleminckx et al. 2021). Missing trait data ranged from 34.96% for leaf thickness up to 74.17%
270 for root SRL (see Table S2 in Vleminckx et al. 2021). Missing values were imputed using a
271 Bayesian hierarchical matrix factorization method (BHMF), based on taxonomic information
272 and co-variation among traits (Fazayeli et al. 2014; see Vleminckx et al. 2021 for details). All
273 these traits reflect species economics spectrum potentially associated to soil nutrient availability
274 levels, or intrinsic water-use efficiency (Leaf ^{13}C) (Baraloto et al. 2010).

275

276 **Data analysis**

277 *Niche breadth and niche position data*

278 Species abundance at the plot level was calculated after weighting each tree by the
279 logarithm of its basal area, to take into account that later life stages are likely to be more
280 representative of the influence of habitat conditions on species distributions, whereas the
281 assembly rules of younger trees can be more stochastic (Vleminckx et al. 2015). We then
282 calculated the niche breadth and the niche position of each of the 246 species that were present
283 in at least three subregions (i.e., areas comprising plots), across each of the five soil nutrients
284 (N, P, Ca, Mg and K). For each soil variable, the niche position of each species corresponded
285 to the median of the soil variable calculated among plots where the species was found
286 (weighting each plot according to the abundance of the species). The niche breadth was
287 calculated as the interquartile range (25-75%) of values for the soil variable. The 25-75% range
288 was chosen to provide robust niche breadth values that were weakly sensitive to outliers
289 (Steidinger 2015). Calculations using a 20-80% and a 15-85% range provided highly consistent
290 results that did not modify our interpretations. Prior to any subsequent analysis, niche breadth
291 and niche position values were normalized (using a Box-Cox transformation) and standardized
292 (z-score transformation). We then detrended niche breadth values to remove any potential

293 biased inflation of these values induced by the effects of: (i) the total abundance of each species
294 across all plots, (ii) the number of subregions and (iii) plots in which each species is present,
295 and (iv) their regional distribution (i.e. dummy variable columns indicating whether each
296 species is present in one region, i.e. Western or Eastern Amazon, or both regions). This
297 detrending was performed by using the residuals of a linear regression of niche breadth against
298 these effects (see details in Appendix S4).

299 *Niche breadth and niche position correlations among soil variables*

300 To specifically address question 1, we performed a PCA on the species niche breadth
301 values corresponding to the different soil nutrients, and the same PCA for species niche position
302 values. We then tested whether the Pearson correlations of niche breadth and niche position
303 among the five soil nutrients were statistically significant. Correlations were considered
304 significant when they were lower or higher than the 2.5-97.5% quantiles of correlation values
305 obtained after randomizing each nutrient concentration values at the plot level and recalculating
306 niche breadth and niche position, while preserving the multi-scale spatial structure of each
307 nutrient within each study region (Peru and French Guiana), independently. To do so, we used
308 Moran Spectral Randomization (MSR, [Wagner and Dray 2015](#)), a procedure that allows
309 considering multiscale spatial autocorrelation structures for any type of quantitative variable,
310 based on spatially weighted connectivity information among sampling points (i.e. the 101 plots
311 in our case). This information was obtained from an optimized procedure used to choose a
312 spatial weighted matrix and select a subset of Moran's eigenvector maps (MEMs, [Dray et al.](#)
313 [2006](#)), following [Bauman et al. \(2018a,b\)](#), using the R package 'adespatial' ([Dray et al. 2022](#)).
314 MEMs are spatial eigenvectors that model multi-scale spatial structures in any type of
315 numerical variable. We tested a minimum spanning tree configuration and a Gabriel's graph to
316 model connectivity among plots, which have been shown appropriate to accurately modeling
317 structures even when dealing with nested and irregular sampling designs such as ours ([Bauman](#)

318 [et al. 2018a](#)). The spatial weighted connectivity information from the best MEM model (i.e.,
319 the eigenvector combination that best described the spatial structures in the soils nutrients'
320 concentration, based on a forward selection with double stopping criterion) is then used in a
321 spatially constrained randomization algorithm in the MSR method to reproduce variables that
322 accurately mimic the observed spatial structures of the randomized variable(s).

323 Species in each PCA graph were also characterized by their affinity for each of the three
324 habitats, by calculating and testing their indicator value (indval), following Dufrêne & Legendre
325 (1997). This allowed combining quantitative soil information with qualitative visualization of
326 three well-defined and contrasted habitats of the Amazon region (white-sand, terra firme and
327 seasonally flooded).

328 *Relationship between niche optimum, niche breadth and traits for each soil nutrient*

329 To address question 2, we plotted the niche breadth of species against their niche
330 position values, for each soil variable. The linear and non-linear relationships between niche
331 breadth and niche position were fitted using Bayesian regression models. The posterior
332 distributions of the slope coefficients of interest were summarized through the median and 95%
333 posterior credibility interval. The linear and non-linear (quadratic) slope coefficient
334 distributions were fitted (Bayesian updating) using a quadratic approximation ([McElreath](#)
335 [2020](#)). The shape of the niche breadth-position associations and the importance of the linear
336 and quadratic coefficients were used to verify which scenario in Fig. 1 best fits the observed
337 niche breadth-position relationship, for each soil nutrient. Coefficient values were considered
338 as clearly positive or negative whenever at least 95% of their posterior mass probability was
339 positive or negative (i.e., did not encompass zero). Scenarios 2 and 3 predict positive values for
340 the linear coefficient and non-important values for scenarios 1 and 4. Scenarios 3 and 4 predict
341 negative values for the quadratic coefficient, while the latter is expected to be non-important
342 for scenarios 1 and 2.

343 To address question 3, we performed a variation partitioning to quantify, for each soil
344 variable, the fraction (adjusted R^2) of species niche breadth variation explained purely by their
345 niche position and by their functional traits. We then tested the significance of each fraction by
346 testing whether the observed fraction (adjusted R^2 values) was higher than 95% of null values
347 obtained with the MSR method described above. If the observed adjusted R^2 value quantifying
348 the effect of all traits combined was higher than 95 % of the 4999 adjusted R^2 values obtained
349 with the MSR procedure, then we performed a forward selection to identify the traits that
350 significantly explained niche breadth variation (Blanchet et al. 2008).

351 Prior to the variation partitioning, we verified whether niche breadth values were
352 influenced by phylogeny. Phylogeny was modelled using a matrix of dummy variables
353 assigning “1” for each species (lines) in their corresponding genus and family (in columns), and
354 “0” for non-matching taxa. The phylogenetic effect was then tested using a residuals
355 permutation test (Anderson and Legendre 1999), which showed no significant effect for any
356 soil variable (Appendix S5: Table S1).

357 All analyses described in the methods were performed in the R statistical environment
358 (R Development Core Team, 2022). We provide the soil, tree inventory and trait data, along
359 with our R script in the online repository folder: <https://doi.org/10.7910/DVN/VWAJYR>.
360 References for the R packages used are detailed in the R code.

361 **Results**

362 **Correlation of niche breadths and positions among soil variables**

363 The two PCAs performed on niche breadth and niche position values showed highly
364 consistent patterns of variables’ projection, revealing a strong relationship between these two
365 niche parameters (Procrustes correlation = 0.587; $P \leq 0.001$; MSR test; Fig. 3). There was a
366 strong coordination of species niche breadth and position for soil cations (Ca, Mg and K) and
367 to a lesser extent for N. Increasing niche breadth and position values for N, Ca, Mg and K

368 aligned well with increasingly acquisitive functional traits such as higher leaf N concentration
369 (Fig. 3). Soil P concentration showed a clear decoupling of niche breadth and position values
370 compared to the other nutrients (Fig. 3). Species significantly indicative of seasonally flooded
371 and terra firme habitats displayed significantly higher niche breadth and niche position, as well
372 as higher leaf N and P concentration for soil N, Ca, Mg and K concentration, compared to white-
373 sand specialists, (Appendix S6: Figure S1, and Appendix S7: Figure S1; for sample size details,
374 see Appendix S8: Figure S1). The following analyses examine in more details the relationship
375 between niche breadth, niche position and functional traits for each soil nutrient.

376

377 **Functional strategies associated with niche breadth and position**

378 Species niche breadth was positively associated with niche position for each of the five
379 soil nutrients (Fig. 4). No clear negative quadratic term was detected for niche position,
380 indicating that relationships were mostly linear and consistent with scenario 2 (Fig. 1). The
381 niche breadth-position linear relationship was the strongest for soil Ca concentration (R^2 value
382 = 45.1%), followed by soil N (40.2%), P (26.2%) and K (18.2%) concentration. The effect of
383 functional traits on niche breadth nearly entirely co-varied with the effect of niche position. In
384 other words, we did not observe any trait explaining species niche breadth alone. Niche breadth
385 and position values were not significantly explained by the genus and family identity of species
386 for any soil variable ($R^2 < 1\%$; Appendix S5: Table S1).

387 Functional traits contributed to species niche breadth ($P \leq 0.05$; MSR test) for soil N
388 ($R^2 = 3.7\%$) and Ca (12.4%) concentration, with high niche breadth values for these two soil
389 nutrients being associated with more resource acquisitive strategies among species, in particular
390 higher SLA, Leaf N and Ca concentrations, and higher fine root SRL (Fig. 4). The Pearson
391 correlations between each individual trait and species niche breadth for soil N, Ca, Mg and P
392 concentration are shown in supplementary material (Appendix S9: Figure S1). Species niche

393 breadth for soil K concentration was not significantly explained by functional traits (Fig. 4).
394 Results obtained with soil Mg concentration were consistent with the ones obtained with soil
395 Ca concentration (Appendix S10: Figure S1). Functional traits less clearly explained the niche
396 breadth of soil P ($R^2=1.9\%$), although sapwood density was retained by the forward selection
397 procedure, with species distributed on the most P-depleted soils showing denser wood than on
398 less P-limiting conditions.

399 **Discussion**

400 Niche properties, characterized by species range (niche breadth) and optimum (niche position)
401 along soil nutrient gradients, were coordinated among soil N, Ca, Mg and K, but not soil P
402 (Fig. 3). The decoupling of species niches between soil P concentration and the other nutrients
403 was associated with different functional strategies (Fig. 4). Our results suggest that species
404 undergo increasing abiotic constraints that favor costly resource conservation strategies when
405 soil fertility decreases. These abiotic constraints decrease with increasing soil fertility,
406 allowing species exhibiting more resource acquisitive traits to occupy increasingly larger
407 niches, in line with scenario 2 (Fig. 1).

408 **Costly poor-soil adaptations limit species edaphic ranges**

409 We found a strong positive and linear increase of species niche breadth with their niche
410 position, for each soil nutrient (Fig. 3, 4), in contrast with predictions from scenario 1. The
411 quadratic term of the niche breadth-position relationship was never clearly different from zero
412 and always positive, which invalidated scenarios 3 and 4 and provided support for scenario 2.
413 Although our sampling may not have captured the full edaphic distribution for every species,
414 the gradients that we measured and the care with which we effected taxonomic determinations,
415 represent a nearly complete picture for most of these species' distributions (Quesada et al. 2010,
416 Baraloto et al. 2021), such that additional sampling would be unlikely to change the present
417 results. It is also worth noting that the way we accounted for spatial distribution disparities

418 among species in the analyses strongly limited the potential influences of spatial biases related
419 to the statistical design (Taylor 1961).

420 Species distributed on the most N and Ca-depleted soils had lower leaf nutrient
421 concentrations, in particular N and Ca, while also showing relatively low SLA (Fig. 4,
422 Appendix S7: Figure S1), indicating resource conservation strategies (Fortunel et al. 2014).
423 These species also displayed relatively low niche breadth values, which may suggest that their
424 resource conservation traits confine them to these poor soil conditions (generally white-sands),
425 and exclude them from the more fertile terra firme and seasonally flooded soils.

426 The positive association between species niche breadth for soil Ca concentration and
427 SRL may reflect the existence of a fast-slow trade-off associated with soil fertility conditions,
428 with poor soils occupied by species investing in longer roots with lower tissue quality, possibly
429 associated with higher uptake capacity in more competitive environments. Our results may
430 suggest that soil Ca limitation has had more influence than the four other soil nutrients studied
431 here on fine root evolutionary history and is consistent with previous manipulative studies in
432 tropical Amazonian forests (Wurzburger & Wright 2015). Nevertheless, root traits were
433 generally poor predictors of niche breadth, possibly because of the multiple alternatives that
434 plants use for nutrient capture, including investments in mycorrhizal associations, that make
435 possible a wide spectrum of trait syndromes in the same soil conditions (Valverde-Barrantes et
436 al. 2017).

437 The niche breadth-position relationship was significantly positive but relatively weaker
438 for soil K concentration ($R^2 = 18.2\%$) than for soil Ca, N and P concentration ($\geq 26.2\%$; Fig.
439 4). Yet, niche position and niche breadth for soil K concentration did not show any significant
440 association with any functional trait, contrary to the three other soil nutrients. Thus, while our
441 results suggest that K may indeed limit primary productivity, which is consistent with previous
442 studies in lowland tropical forests (Wright et al. 2011, Baribault et al. 2012, Santiago et al.

443 2012), they also nuance the idea that single functional traits reflect edaphic adaptations among
444 tree species. The decoupling of fast-slow economic spectra reported among Amazonian tree
445 communities (Baraloto et al. 2010, Fortunel et al. 2012, Vleminckx et al. 2021) may partly
446 introduce statistical noise when testing a signal between a single trait and a soil variable, and
447 thus partly explains the weak predictive power of traits on species niche breadth.

448 The marked niche breadth-position relationship observed for soil P ($R^2 = 26.2\%$) was
449 highly decoupled from the other four soil nutrients (Fig. 3, 4). This pattern was consistent with
450 the orthogonality between soil P variation and the four other soil nutrients (Appendix S3: Figure
451 S1). This orthogonality supports previous evidence that soil P availability often varies
452 independently from cationic nutrients (Ca, Mg, K) or can even be higher on cation-poor sandy
453 soils, due to the immobilization of P into Al oxyhydroxide complex forms in more fertile,
454 clayey tropical soils (Walker & Syers 1976, Vleminckx et al. 2015, Turner 2018, Cunha et al.
455 2022). In fact, P availability was even higher on white-sand forests than on the other edaphic
456 habitats in Peru (Table 2), whereas the reverse pattern was observed in French Guiana. Yet, the
457 overall niche breadth-position correlation remained strongly positive, even when considering
458 the disparities of habitat differences for P availability across regions.

459 The decoupling of niche dimensions between soil P and the other four soil nutrients was
460 associated with different functional dimensions. More specifically, species preferences for terra
461 firme and seasonally flooded soils, which contained the highest soil N and cation
462 concentrations, were mostly reflected by acquisitive traits in the leaves, whereas species whose
463 optimum was on low P availability soils tended to have denser wood. The latter signal was
464 weak but nevertheless significant (Fig. 4), and while further studies are needed to verify
465 consistent patterns, it may partly explain the decoupling of traits that has previously been
466 reported among leaf and woody aboveground organs when measured across broad edaphic
467 gradients (Baraloto et al. 2010, Fortunel et al. 2014, Vleminckx et al. 2021).

468 In parallel with using combinations of forward-selected traits in the variation
469 partitioning, we also followed the approach of previous studies which examined the association
470 between functional strategies and species niche parameters by using multivariate functional
471 variables ([Kraft et al. 2015](#), [Muscarella et al. 2016](#), [Pistón et al. 2019](#)). This multivariate trait
472 approach was generally less predictive than the forward-selected trait approach shown in Fig.
473 4 (for more details, see Appendix S11: Figure S1 and Figure S2).

474 The overall effect of functional traits on niche breadth variation co-varied with the effect
475 of niche position (Fig. 4). This suggests that the resource use traits studied here mostly reflect
476 species edaphic optima and not their range of resource use. It is also worth noting that intra-
477 specific trait variation may have partly limited the detection of niche-trait association at the
478 species level ([Zuleta et al. 2022](#)), but we lack enough trait measurements across habitats for
479 each species to have more accurate insights.

480 Finally, the absence of genus or family-level signal on niche breadth and position
481 (Appendix S5: Table S1) may suggest that various edaphic niches have evolved multiple times
482 within many different genera and families, which is consistent with recent reports ([Fine and](#)
483 [Baraloto 2016](#), [Baraloto et al. 2021](#)).

484 Our results provide further support for the determinant role of soil properties in shaping
485 tree species assembly in tropical forests ([Russo et al. 2005](#), [Condit et al. 2013](#), [Vleminckx et al.](#)
486 [2017](#), [Wright et al. 2019](#), [Umaña et al. 2021](#)), while they also provide indirect support to the
487 hypothesis that the strength of abiotic filtering, here mediated by soil nutrient contents,
488 determines the degree of species habitat specialization, i.e. to what extent species are confined
489 to smaller niches because of their costly investments in resource conservation that would
490 potentially make them less competitive in more fertile habitats. Definitive evidence of
491 competitive exclusion would further require adding a temporal dimension to these analyses –
492 i.e. tree demography –, for instance relating tree growth or mortality responses to the interplay

493 of soil, traits, and the functional similarity of the neighborhood (Fortunel et al. 2016, Muledi et
494 al. 2020, Rozendaal et al. 2020). Such dynamics data unfortunately remain too scarce in the
495 tropics for accurate characterization of demographic parameters for many species across the
496 breadth of their distribution ranges, emphasizing the need for continued efforts towards
497 establishing and monitoring long-term permanent sample plots in the tropics (Blundo et al.
498 2021, Davies et al. 2021).

499 Here, we did not investigate the possibility that the steep nutrient gradient occurring
500 across habitat may overlap with a gradient of forest dynamics. Canopy disturbance and forest
501 turnover rate are likely greater in the most fertile habitats (Baraloto et al. 2011, Baker et al.
502 2014), with more productive tree communities exhibiting more acquisitive traits (e.g., high
503 SLA, low leaf thickness...) for soil nutrients and light (Fortunel et al. 2014, Vleminckx et al.
504 2020, 2021). A greater light extinction profile is also expected on fertile soils (Russo et al.
505 2012), which may limit the competitiveness of fast-growing species in the understory, although
506 this effect might be compensated by lower air evaporative demand and thermal constraints
507 (Vinod et al. 2022) in the more shaded vegetation strata. Accurate gap dynamics history and
508 light availability data will need to be better studied to further examine how light and soil nutrient
509 gradients interact to influence niche parameters.

510

511 **Implications regarding forest conservation and tree responses to climate change**

512 Species adapted to poor soil conditions likely have large potential edaphic niches
513 compared to their realized one, as they could in theory thrive on a much wider range of soil
514 fertilities in the absence of faster-growing competitors, unlike species with higher niche fertility
515 optimum whose realized and fundamental niches are expected to be more packed. The costly
516 resource conservation traits displayed by poor-soil specialists are likely to exclude them from
517 more fertile habitats, explaining the disparities between their realized and fundamental niches.

518 These adaptations might also allow these species to extend their tolerance to other
519 environmental constraints such as water deficiency (Baraloto et al. 2010), which occurs more
520 frequently on highly drained white-sands than on terra firme or seasonally flooded soils. This
521 would potentially render white-sand tree communities more resilient to more prolonged dry
522 seasons and temperature increases predicted by climate models, predictions that are particularly
523 threatening in the North-Eastern Amazon (Fortunel et al. 2014, Guevara et al. 2016, Esquivel-
524 Muelbert et al. 2018, IPCC 2022). These results could also pave the way for developing more
525 evidence-based forest restoration management plans, for instance by improving the selection of
526 tree species that would be able to establish in a wide range of environmental conditions. Further
527 investigations of the interplay of species niche breadth, niche position and functional strategies
528 for complementary key edaphic and climatic niche dimensions and across different tropical
529 regions and spatial scales will be urgently needed to better predict how the current context of
530 rapid environmental changes is likely to affect tropical forest species composition and
531 associated ecosystem functions.

532

533 4. Acknowledgments

534 JV is a postdoctoral fellow funded by a G. Evelyn Hutchinson Environmental Postdoctoral
535 Fellowship from the Yale Institute for Biospheric Studies (Yale University, CT, USA). DB was
536 funded by the European Union's Horizon 2020 research and innovation program under the
537 Marie Skłodowska-Curie grant agreement No. 895799. This work was supported by
538 collaborative research grants funded by “Investissement d’Avenir” grants of the ANR
539 (CEBA:ANR-10-LABX-25-01); by the National Science Foundation (NSF) grant DEB-
540 0743103/0743800 to CB and PVAF; by ANR Blanc NEBEDIV (Projet ANR-13-BSV7-009)
541 and an INRAE Package grant to CB; and by NSF DEB 1254214 to PVAF.

542 5. Author Contributions

543 C.B. and P.V.A.F. were co-principal investigators for the projects that supported this research.
544 The collection and identification of tree species was coordinated by C.B and P.V.A.F., with
545 help of J.E., P.P., N.D., M.R., E.V., I.M., J.G., C.F., E.A., T.P., A.D., J-Y.G., O.V.B., F.D. and
546 J.V. J.V., C.F., O.V.B. and C.B. led the trait data collection in French Guiana and Peru. J.V.
547 analyzed the data, with help from D.B. with Bayesian analyses. J.V. led the writing of the
548 manuscript. C.B., O.V.B., C.F. and D.B. commented on early versions of the manuscript. All
549 authors contributed to the preparation of the final manuscript.

550 6. Conflict of Interest Statement

551 The authors declare no conflict of interest

552 7. Literature cited

553 Anderson, M. J. and Legendre, P. 1999. An empirical comparison of permutation methods for
554 tests of partial regression coefficients in a linear model. – *J. Stat. Comput. Sim.* 62: 271–
555 303.

556 Asefa, M., Samantha J, W., Cao, M., Xiaoyang, S., Yudi M, L., & Jie, Y. 2022. Above and
557 belowground plant traits are not consistent in response to drought and competition
558 treatments. *Annals of Botany*. <https://doi.org/10.1093/aob/mcac108>

559 Baker, T. R., et al. 2014. Fast demographic traits promote high diversification rates of
560 Amazonian trees. *Ecology Letters* 17:527–536.

561 Baraloto, C. et al. 2010. Decoupled leaf and stem economics in rain forest trees. – *Ecol. Lett.*
562 13: 1338–1347.

563 Baraloto, C., Rabaud, S., Molto, Q., Blanc, L., Fortunel, C., Herault, B., ... & Fine, P. V. 2011.
564 Disentangling stand and environmental correlates of aboveground biomass in
565 Amazonian forests. *Global Change Biology*, 17(8), 2677-2688.

566 Baraloto, C. et al. 2013. Rapid simultaneous estimation of aboveground biomass and tree
567 diversity across Neotropical forests: a comparison of field inventory methods. –
568 *Biotropica* 45: 288–298.

569 Baraloto, C., Vleminckx, J., Engel, J., Petronelli, P., Dávila, N., Ríos, M., Valderrama
570 Sandoval, E. H., Mesones, I., Guevara Andino, J. E., Fortunel, C., Allie, E., Paine, C.
571 E. T., Dourdain, A., Goret, J.-Y., Valverde-Barrantes, O. J., Draper, F., and Fine, P. V.
572 A. 2021. Biogeographic history and habitat specialization shape floristic and
573 phylogenetic composition across Amazonian forests. *Ecological Monographs*
574 91(4):e01473. 10.1002/ecm.1473

575 Baribault, T.W., Kobe, R.K. & Finley, A.O. (2012). Tropical tree growth is correlated with soil
576 phosphorus, potassium, and calcium, though not for legumes. *Ecol. Monogr.*, 82, 189–
577 203.

578 Bauman, D., T. Drouet, M. J. Fortin, and S. Dray. 2018a. Optimizing the choice of a spatial
579 weighting matrix in eigenvector-based methods. *Ecology* 99:2159–2166.

580 Bauman, D., T. Drouet, S. Dray, and J. Vleminckx. 2018b. Disentangling good from bad
581 practices in the selection of spatial or phylogenetic eigenvectors. *Ecography* 41:1–12.

582 Blanchet, F. G., P. Legendre, and D. Borcard. 2008. Forward selection of explanatory variables.
583 *Ecology* 89:2623–2632.

584 Blundo, C., Carilla, J., Grau, R., Malizia, A., Malizia, L., Osinaga-Acosta, O., ... & De Araujo,
585 R. O. (2021). Taking the pulse of Earth's tropical forests using networks of highly
586 distributed plots. *Biological Conservation*, 260, 108849.

587 Carscadden, K. A., Emery, N. C., Arnillas, C. A., Cadotte, M. W., Afkhami, M. E., Gravel, D.,
588 Livingstone, S. W., & Wiens, J. J. (2020). Niche breadth: Causes and consequences for
589 ecology, evolution, and conservation. *The Quarterly Review of Biology*, 95(3), 179–
590 214

591 Condit, R., B. M. J. Engelbrecht, D. Pino, R. Perez, and B. L. Turner. 2013. Species
592 distributions in response to individual soil nutrients and seasonal drought across a
593 community of tropical trees. *Proceedings of the National Academy of Sciences of the*
594 *United States of America* 110:5064–5068.

595 Cunha, H. F. V., Andersen, K. M., Lugli, L. F. et al. (2022) Direct evidence for phosphorus
596 limitation on Amazon forest productivity. *Nature* 608, 558–562.

597 Dauby, G., and O. J. Hardy. 2011. Sampled-based estimation of diversity sensu stricto by
598 transforming Hurlbert diversities into effective number of species. *Ecography* 34:001–
599 012.

600 Davies, S. J., Abiem, I., Salim, K. A., Aguilar, S., Allen, D., Alonso, A., ... & Yap, S. L. (2021).
601 ForestGEO: Understanding forest diversity and dynamics through a global observatory
602 network. *Biological Conservation*, 253, 108907.

603 Dray, S. et al. 2006. Spatial modelling: a comprehensive framework for principal coordinate
604 analysis of neighbour matrices (PCNM). – *Ecol. Model.* 196: 483–493.

605 Dray, S., Bauman, D., Blanchet, G., Borcard, D., Clappe, S., Guénard, G., Jombart, T.,
606 Larocque, G., Legendre, P., Madi, N., Wagner, H.H. (2022) *adespatial: Multivariate*
607 *Multiscale Spatial Analysis*. R package version 0.3-14. [https://CRAN.R-](https://CRAN.R-project.org/package=adespatial)
608 [project.org/package=adespatial](https://CRAN.R-project.org/package=adespatial)

609 Dobzhansky T. 1950. Evolution in the tropics. *Am. Sci.* 38:209–21.

610 Dufrene, M., and P. Legendre. 1997. Species assemblages and indicator species: the need for a
611 flexible asymmetrical approach. *Ecological Monographs* 67:345–366.

612 Esquivel-Muelbert, A., et al. 2018. Compositional response of Amazon forests to climate
613 change. *Global Change Biology* 25:39–56.

614 Fazayeli, F. et al. 2014. Uncertainty quantified matrix completion using Bayesian hierarchical
615 matrix factorization. – *Int. Conf. on Machine Learning and Applications (ICMLA)*.

616 Fine, P. V. A., Miller, Z. J., Mesones, I., Irazuzta, S., Appel, H. M., Stevens, M. H., et al. (2006).
617 The growth-defense trade-off and habitat specialization by plants in Amazonian forests.
618 Ecology 87, 150–162.

619 Fine, P.V.A., García-Villacorta, R., Pitman, N.C.A., Mesones, I. & Kembel, S.W. (2010).
620 Floristic Study of the White-Sand Forests of Peru," Annals of the Missouri Botanical
621 Garden 97(3), 283-305.

622 Fine, P. V. A., Metz, M. R., Lokvam, J., Mesones, I., Ayarza Zuniga, J. M., Lamarre, G. P. A.,
623 et al. (2013). Insect herbivores, chemical innovation and the evolution of habitat
624 specialization in Amazonian trees. Ecology 94, 1764–1775.

625 Fine, P. V. A., and C. Baraloto. (2016). Habitat endemism in white-sand forests: insights into
626 the mechanisms of lineage diversification and community assembly of the Neotropical
627 flora. Biotropica 48:24–33.

628 Fortunel, C. et al. 2012. Leaf, stem and root tissue strategies across 758 Neotropical tree species.
629 – Funct. Ecol. 26: 1153–1161.

630 Fortunel, C., C. E. T. Paine, P. V. A. Fine, N. J. B. Kraft, and C. Baraloto. 2014. Environmental
631 factors predict community functional composition in Amazonian forests. Journal of
632 Ecology 102:145–155.

633 Fortunel, C., Valencia, R., Wright, S.J., Garwood, N.C. and Kraft, N.J.B. (2016), Functional
634 trait differences influence neighbourhood interactions in a hyperdiverse Amazonian
635 forest. Ecol Lett, 19: 1062-1070.

636 Futuyma D. J., Moreno G. 1988. The evolution of ecological specialization. Annual Review of
637 Ecology, Evolution, and Systematics 19:207–233.

638 Guevara, J. E., et al. 2016. Low phylogenetic beta diversity and geographic neo-endemism in
639 Amazonian white-sand forests. Biotropica 48:34–46.

640 Gourlet-Fleury, S. et al. 2004. Ecology and management of a neotropical rainforest: lessons
641 drawn from Paracou, a long-term experimental research site in French Guiana (Gourlet-
642 Fleury, S. et al., eds). – Elsevier.

643 Hedin LO, Brookshire ENJ, Menge DNL, Barron AR. 2009 The nitrogen paradox in tropical
644 forest ecosystems. *Annu. Rev. Ecol. Syst.* 40, 613–635

645 Hoorn, C., et al. 2010. Amazonia through time: Andean uplift, climate change, landscape
646 evolution, and biodiversity. *Science* 330:927–931.

647 Hubbell, S. P. 2001. A unified neutral theory of biodiversity and biogeography. Princeton
648 University Press, Princeton, New Jersey, USA.

649 Hutchinson, G. E. (1957). Concluding remarks. *Cold Springs Harbor Symposium in*
650 *Quantitative Biology*, 22, 415–427. <https://doi.org/10.1101/SQB.1957.022.01.039>

651 IPCC, 2022: Climate Change 2022: Impacts, Adaptation and Vulnerability. Contribution of
652 Working Group II to the Sixth Assessment Report of the Intergovernmental Panel on
653 Climate Change [H.-O. Pörtner, D.C. Roberts, M. Tignor, E.S. Poloczanska, K.
654 Mintenbeck, A. Alegría, M. Craig, S. Langsdorf, S. Löschke, V. Möller, A. Okem, B.
655 Rama (eds.)]. Cambridge University Press. Cambridge University Press, Cambridge,
656 UK and New York, NY, USA, 3056 pp., doi:10.1017/9781009325844.

657 Kraft, N.J.B., Adler, P.B., Godoy, O., James, E.C., Fuller, S. & Levine, J.M. (2014).
658 Community assembly, coexistence and the environmental filtering metaphor. *Funct.*
659 *Ecol.* 29, 592–599.

660 Kraft, N. J., Godoy, O., & Levine, J. M. (2015). Plant functional traits and the multidimensional
661 nature of species coexistence. *Proceedings of the National Academy of Sciences*,
662 112(3), 797-802.

663 Laughlin, D.C. (2014). The intrinsic dimensionality of plant traits and its relevance to
664 community assembly. *J. Ecol.*, 102, 186–193.

665 Le Bagousse-Pinguet, Y., Gross, N., Maestre, F.T., Maire, V., de Bello, F., Fonseca, C.R.,
666 Kattge, J., Valencia, E., Leps, J. and Liancourt, P. (2017), Testing the environmental
667 filtering concept in global drylands. *J Ecol*, 105: 1058-1069.
668 <https://doi.org/10.1111/1365-2745.12735>

669 MacArthur 1969. Patterns of communities in the tropics. *Biological Journal of the Linnean*
670 *Society* 1: 19-30.

671 McElreath, R. (2020). *Statistical rethinking: A Bayesian course with examples in R and Stan*.
672 Chapman and Hall/CRC.

673 McGill, B.J., Enquist, B.J., Weiher, E. & Westoby, M. (2006) Rebuilding community ecology
674 from functional traits. *Trends in Ecology & Evolution*, 21, 178–185.

675 Malanson, G.P., Westman, W.E. & Yan, Y.L. (1992) Realized versus fundamental niche
676 functions in a model of chaparral response to climatic change. *Ecological Modelling*,
677 64, 261–277.

678 Muledi, J., Bauman, D., Jacobs, A., Meerts, P., Shutcha, M., & Drouet, T. (2020). Tree growth,
679 recruitment, and survival in a tropical dry woodland: The importance of soil and
680 functional identity of the neighbourhood. *Forest ecology and management*, 460, 117894.

681 Muscarella, R., & Uriarte, M. (2016). Do community-weighted mean functional traits reflect
682 optimal strategies?. *Proceedings of the Royal Society B: Biological Sciences*,
683 283(1827), 20152434.

684 Phillips, O. L., R. Vásquez Martínez, P. Núñez Vargas, A. Lorenzo Monteagudo, M.-E. Chuspe
685 Zans, W. Galiano Sánchez, A. Peña Cruz, M. Timaná, M. Yli-Halla, and S. Rose. 2003.
686 Efficient plot-based floristic assessment of tropical forests. *Journal of Tropical Ecology*
687 19:629–645.

688 Pianka ER. 1966. Latitudinal gradients in species diversity: a review of the concepts. *Am. Nat.*
689 100:33–46.

690 Pinho, B.X., Melo, F.P.L., Arroyo-Rodríguez, V., Pierce, S., Lohbeck, M., Tabarelli, M. Soil-
691 mediated filtering organizes tree assemblages in regenerating tropical forests. *J Ecol.*
692 2017; 00: 1– 11. <https://doi.org/10.1111/1365-2745.12843>

693 Pistón, N., de Bello, F., Dias, A.T.C., et al. (2019) Multidimensional ecological analyses
694 demonstrate how interactions between functional traits shape fitness and life history
695 strategies. *Journal of Ecology* 107: 2317–2328. [https://doi.org/10.1111/1365-](https://doi.org/10.1111/1365-2745.13190)
696 [2745.13190](https://doi.org/10.1111/1365-2745.13190)

697 Poorter, L., Castilho, C.V., Schiatti, J., Oliveira, R.S. and Costa, F.R.C. (2018), Can traits
698 predict individual growth performance? A test in a hyperdiverse tropical forest. *New*
699 *Phytol*, 219: 109-121. doi:10.1111/nph.15206

700 Quesada, C. A., Lloyd, J., Schwarz, M., Patiño, S., Baker, T. R., Czimczik, C., ... & Paiva, R.
701 (2010). Variations in chemical and physical properties of Amazon forest soils in relation
702 to their genesis. *Biogeosciences*, 7(5), 1515–1541.

703 R Development Core Team. 2022. R: a language and environment for statistical computing. R
704 Foundation for Statistical Computing, Vienna, Austria. www.R-project.org

705 Reich, P. B. 2014. The world-wide ‘fast–slow’ plant economics spectrum: a traits manifesto. –
706 *J. Ecol.* 102: 275–301.

707 Roughgarden J. 1974. Niche width: biogeographic patterns among *Anolis* lizard populations.
708 *American Naturalist* 108:429–442.

709 Rozendaal, D. M., Phillips, O. L., Lewis, S. L., Affum-Baffoe, K., Alvarez-Davila, E., Andrade,
710 A., ... & Vanderwel, M. C. (2020). Competition influences tree growth, but not
711 mortality, across environmental gradients in Amazonia and tropical Africa. *Ecology*,
712 101(7), e03052.

713 Russo, S.E., Davies, S.J., King, D.A. & Tan, S. (2005) Soil-related performance variation and
714 distributions of tree species in a Bornean Rain Forest. *Journal of Ecology*, 93, 879–889.

715 Russo, S., Zhang, L., & Tan, S. (2012). Covariation between understorey light environments
716 and soil resources in Bornean mixed dipterocarp rain forest. *Journal of Tropical*
717 *Ecology*, 28(1), 33-44. doi:10.1017/S0266467411000538

718 Santiago LS, Wright SJ, Harms KE, Yavitt JB, Korine C, Garcia MN, Turner BL (2012)
719 Tropical tree seedling growth responses to nitrogen, phosphorus and potassium addition.
720 *J Ecol* 100:309–316.

721 Sexton, J. P., Montiel, J., Shay, J. E., Stephens, M. R. and Slatyer, R. A. (2017) Evolution of
722 Ecological Niche Breadth. *Annual Review of Ecology, Evolution, and Systematics* 2017
723 48:1, 183-206.

724 Sheth, S. N., Morueta-Holme, N. & Angert, A. L. Determinants of geographic range size in
725 plants. *New Phytologist* 226: 650–665.

726 Steidinger, B. (2015). Qualitative differences in tree species distributions along soil chemical
727 gradients give clues to the mechanisms of specialization: why boron may be the most
728 important soil nutrient at Barro Colorado Island. *New Phytologist*, 27, 206(3):895-899.

729 Sultan S. E., Wilczek A. M., Hann S. D., Brosi B. J. 1998. Contrasting ecological breadth of
730 co-occurring annual *Polygonum* species. *Journal of Ecology* 86:363–383.

731 Taylor, L. (1961) Aggregation, Variance and the Mean. *Nature* 189, 732–735.

732 Treurnicht, M., Pagel, J., Tonnabel, J., Esler, K.J., Slingsby, J.A. & Schurr, F.M. (2019)
733 Functional traits explain the Hutchinsonian niches of plant species. *Global Ecol*
734 *Biogeogr.* 29: 534–545.

735 Turner, B., Brenes-Arguedas, T. & Condit, R. Pervasive phosphorus limitation of tree species
736 but not communities in tropical forests. *Nature* 555, 367–370 (2018).
737 <https://doi.org/10.1038/nature25789>

738 Umaña, MN, Condit, R, Pérez, R, Turner, BL, Wright, SJ, Comita, LS. (2021) Shifts in
739 taxonomic and functional composition of trees along rainfall and phosphorus gradients
740 in central Panama. *J Ecol.* 109: 51– 61. <https://doi.org/10.1111/1365-2745.13442>

741 Valverde-Barrantes, O. J. et al. 2017. A worldview of root traits: the influence of ancestry,
742 growth form, climate and mycorrhizal association on the functional trait variation of
743 fine-root tissues in seed plants. – *New Phytol.* 215: 1562–1573.

744 Van Breugel, M., D. Craven, H. Ran Lai, M. Baillon, B. L. Turner, J. S. Hall. 2019. Soil
745 nutrients and dispersal limitation shape compositional variation in secondary tropical
746 forests across multiple scales. *Journal of Ecology* 107:566–581.

747 Vinod, N., Slot, M., McGregor, I.R., Ordway, E.M., Smith, M.N., Taylor, T.C., et al. (2022).
748 Thermal sensitivity across forest vertical profiles: patterns, mechanisms, and ecological
749 implications. *New Phytol.*, 237, 22–47.

750 Vleminckx, J., T. Drouet, C. Amani, J. Lisingo, J. Lejoly, and O. J. Hardy. 2015. Impact of
751 fine-scale edaphic heterogeneity on tree species assembly in a central African rainforest.
752 *Journal of Vegetation Science* 26:134–144.

753 Vleminckx, J. et al. 2017. The influence of spatially structured soil properties on tree
754 community assemblages at a landscape scale in the tropical forests of southern
755 Cameroon. – *J. Ecol.* 105: 354–366.

756 Vleminckx, J, Bauman, D, Demanet, M, Hardy, OJ, Doucet, J-L, Drouet, T. Past human
757 disturbances and soil fertility both influence the distribution of light-demanding tree
758 species in a Central African tropical forest. *J Veg Sci.* 2020; 31: 440– 453.
759 <https://doi.org/10.1111/jvs.12861>

760 Vleminckx J, Fortunel C, Valverde-Barranted O, Paine CET, Engel J, Petronelli P, Dourdain
761 AK, Guevara JE, Bérroujon S & Baraloto C (2021) Resolving whole-plant economics

762 from leaf, stem and root traits of 1467 Amazonian tree species. *Oikos*, 130(7): 1193-
763 1208.

764 Vleminckx et al. (2023). Niche breadth of Amazonian trees increases with niche optimum
765 across broad edaphic gradients: Supplementary information provided through the
766 Harvard Dataverse repository: <https://doi.org/10.7910/DVN/VWAJYR>

767 Wagner, H. H., and S. Dray. 2015. Generating spatially constrained null models for irregularly
768 spaced data using Moran spectral randomization methods. *Methods in Ecology &*
769 *Evolution* 6:1169–1178.

770 Walker, T. W. & Syers, J. K. The fate of phosphorus during pedogenesis. *Geoderma* 15, 1–19
771 (1976).

772 Wright SJ, Yavitt JB, Wurzburger N, Turner BI, Tanner EVJ, Sayer EJ, Santiago LS, Kaspari
773 M, Hedin LO, Harms KE, Garcia MN, Corre MD (2011) Potassium, phosphorus, or
774 nitrogen limit root allocation, tree growth, or litter production in a lowland tropical
775 forest. *Ecology* 92:1616–1625. <https://doi.org/10.1890/10-1558.1>

776 Wright, S. J. 2019. Plant responses to nutrient addition experiments conducted in tropical
777 forests. *Ecological Monographs* 89(4):e01382. 10.1002/ecm.1382

778 Wurzburger N, Wright SJ. 2015. Fine-root responses to fertilization reveal multiple nutrient
779 limitation in a lowland tropical forest. *Ecology* 96: 2137–2146.

780 Zuquim, G., Costa, F.R.C., Tuomisto, H. et al. The importance of soils in predicting the future
781 of plant habitat suitability in a tropical forest. *Plant Soil* 450, 151–170 (2020).
782 <https://doi.org/10.1007/s11104-018-03915-9>

783 Zuleta, D., Muller-Landau, H. C., Duque, A., Caro, N., Cardenas, D., Castaño, N., León-Peláez,
784 J. D., & Feeley, K. J. (2022). Interspecific and intraspecific variation of tree branch, leaf
785 and stomatal traits in relation to topography in an aseasonal Amazon forest. *Functional*
786 *Ecology*, 36, 2955– 2968. <https://doi.org/10.1111/1365-2435.14199>

787

788

790 **Table 1.** Summary of key descriptors of study regions, subregions and habitats. NrP = Number
 791 of plots; AR = Altitudinal Range (in m); MAR = Mean Annual Rainfall (in mm); MAT = Mean
 792 Annual Temperature (in °C). NrSp = mean number of species per plot; ENS₂ = mean (calculated
 793 at the plot level) Effective Number of Species expected from 1000 random samplings (with
 794 replacement) of two individuals. The three last lines of each region represent the same
 795 information for each habitat. Numbers in parenthesis correspond to the standard deviation of
 796 the mean.

	NrP	AR	MAR	MAT	NrSp	ENS ₂
<i>French Guiana</i>	64	42-529	2157- 3129	23.0- 26.6	80.3 (3.6)	48.6 (5.2)
<i>Saül-Limonade</i>	12	196-253	2421	24.6	66.1 (4.2)	24.4 (4.5)
<i>Trinité</i>	6	126-320	2671	25.1	112.8 (11.7)	77.8 (14.0)
<i>Itoupé</i>	3	521-529	2530	23.0	79.7 (6.9)	30.1 (7.0)
<i>Mitaraka</i>	9	317-347	2157	24.9	70.8 (10.7)	66.1 (17.2)
<i>Laussat</i>	10	49-57	2402	26.2	74.1 (3.7)	28.0 (4.0)
<i>Nouragues</i>	8	108-345	3328	24.8	86.9 (14.0)	68.0 (20.5)
<i>Petite montagne Tortue</i>	9	47-136	3729	25.4	95.0 (10.5)	66.3 (17.0)
<i>Centre Spatial Guyanais</i>	4	43-63	2932	25.8	76.0 (9.2)	25.3 (5.1)
<i>Kaw</i>	2	254-282	3720	24.5	96.0 (6.0)	73.9 (18.5)
<i>Suriname</i>	2	196-229	2241	26.6	38.5 (3.5)	10.1 (6.3)
<i>Terra Firme</i>	20	45-347	2775	25.2	95.5 (4.4)	70.8 (7.6)
<i>Seasonally Flooded</i>	35	43-529	2723	24.9	64.7 (5.2)	24.5 (4.2)
<i>White Sand</i>	10	39-345	2908	25.7	59.5 (5.6)	21.1 (4.7)
<i>Peru</i>	38	95-173	2405- 2750	26.3- 26.7	101.4 (4.99)	61.2 (6.7)
<i>Morona</i>	6	143-173	2405	26.7	108.2 (6.0)	89.4 (17.2)
<i>North Loreto</i>	18	105-149	2750	26.3	101.6 (8.7)	59.9 (10.5)
<i>South Loreto</i>	14	95-139	2499	26.8	98.3 (7.5)	50.7 (9.0)
<i>Terra Firme</i>	11	95-158	2597	26.6	128.8 (5.6)	101.6 (9.6)
<i>Seasonally Flooded</i>	13	106-156	2636	26.5	87.7 (6.1)	53.4 (9.2)
<i>White Sand</i>	14	106-173	2625	26.6	86.7 (7.8)	29.8 (5.0)

799 **Table 2.** Mean (\pm standard deviation) of each soil variable in each habitat (SF = Seasonally
800 Flooded; TF = Terra Firme; WS = White-Sand) and each study region (French Guiana and
801 Peru).

<i>Habitat</i>	French Guiana			Peru		
	SF	TF	WS	SF	TF	WS
<i>TN (%)</i>	2.29 (3.25)	1.65 (1.35)	0.17 (0.22)	0.23 (0.09)	0.14 (0.05)	0.07 (0.06)
<i>Avail. P (mg/kg)</i>	10.78 (15.51)	5.07 (5.81)	3.67 (4.11)	7.4 (5.75)	2.25 (1.54)	8.4 (8.01)
<i>Ca (mg/kg)</i>	1.26 (2.37)	0.53 (1.02)	0.16 (0.17)	5.96 (7.23)	0.84 (2.58)	0.04 (0.03)
<i>Mg (mg/kg)</i>	0.81 (0.92)	0.32 (0.31)	0.22 (0.24)	1.35 (1.45)	0.31 (0.6)	0.05 (0.04)
<i>K (mg/kg)</i>	0.13 (0.11)	0.1 (0.04)	0.05 (0.05)	0.18 (0.07)	0.06 (0.02)	0.06 (0.03)

802

803

804

805 10. Figure captions

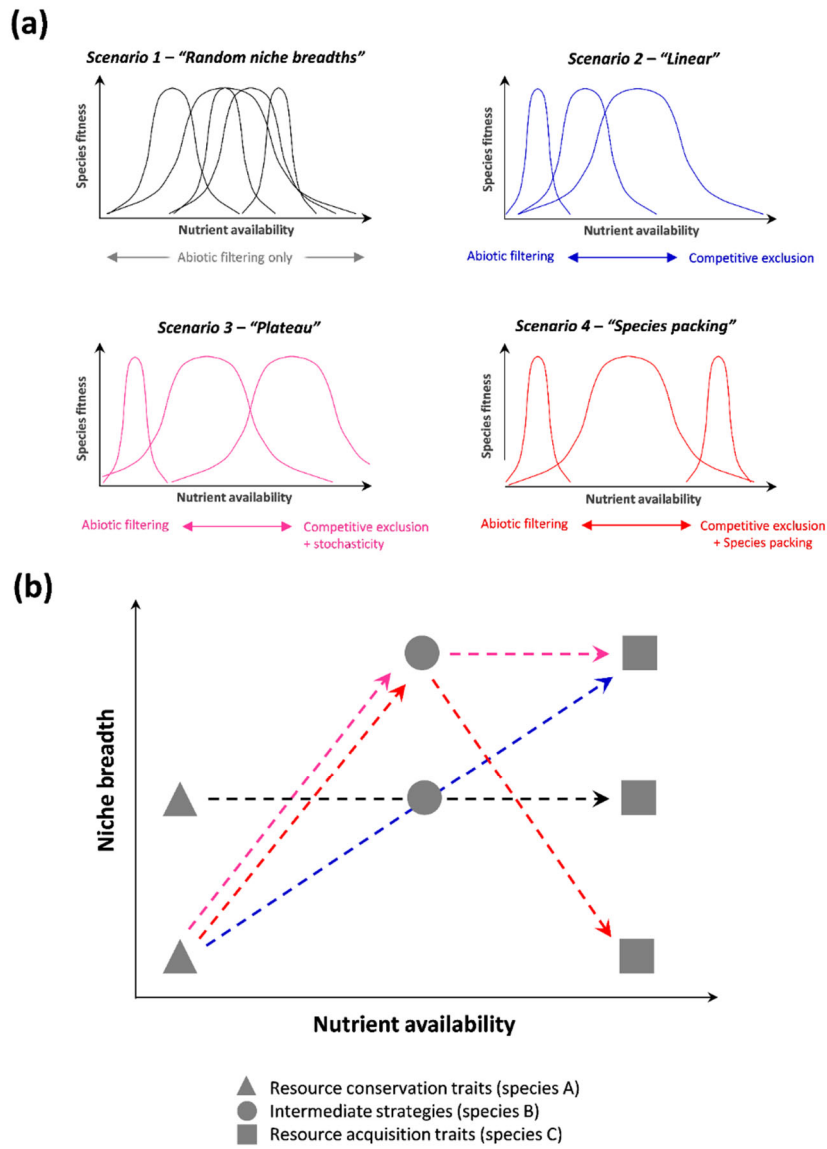
806 **Figure.1** (a) Hypothetical scenarios describing species frequency distributions (realized niches)
807 along a gradient of increasing soil nutrient availability, using Gaussian curves for simplicity.
808 (b) Translation of these scenarios into niche breadth – niche positions graphs, showing species
809 and predicted functional strategies with symbols.

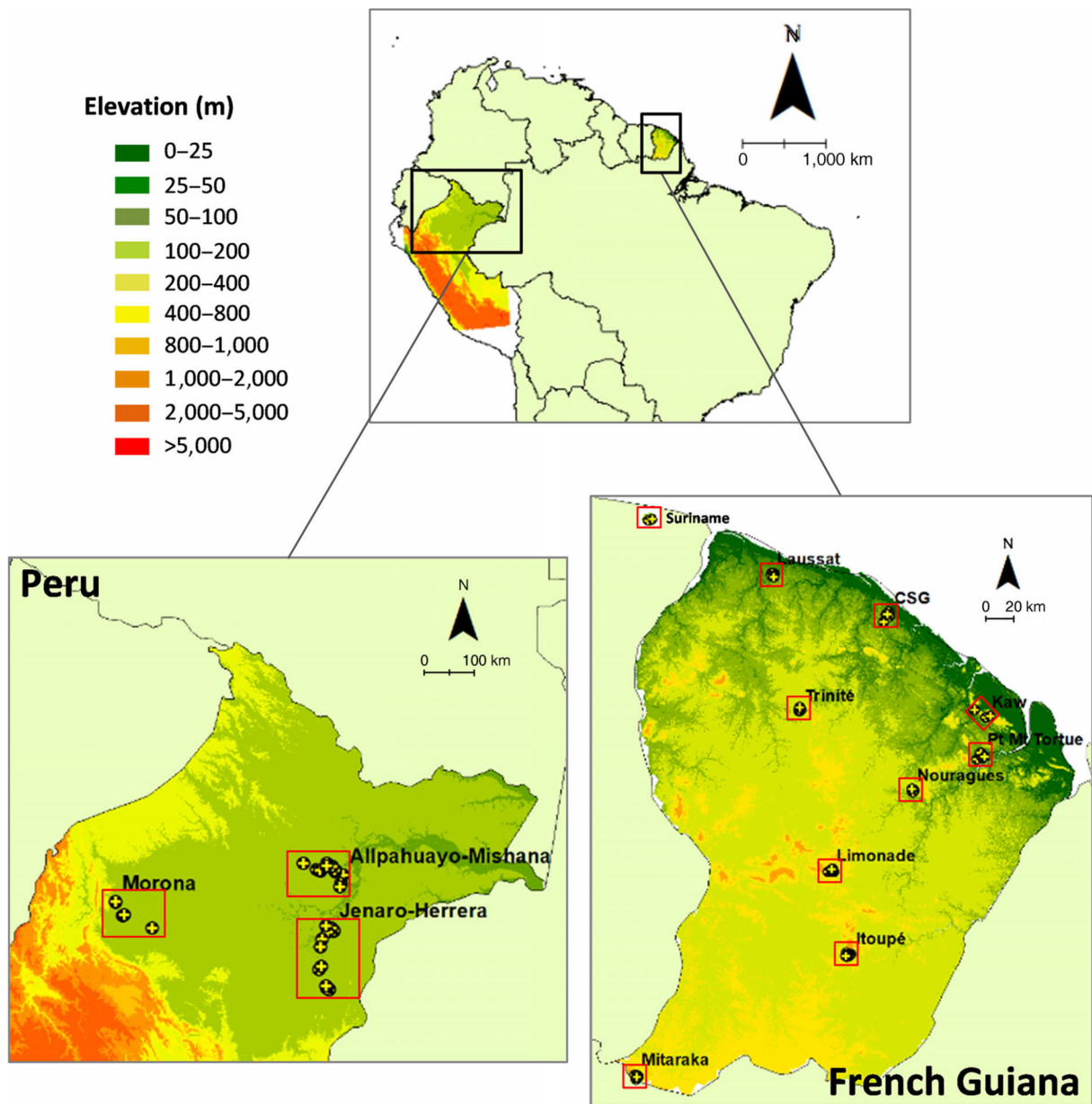
810 **Figure 2.** Geographical distribution of the 13 subregions in the Amazon (red rectangles),
811 showing the position of the plots (yellow cross symbols) within the two study regions (Peru and
812 French Guiana).

813 **Figure 3.** Projection of species and soil variables on axes 1-2 of a principal component analysis
814 (PCA) performed on niche breadth (a) and niche position (b) values. The grey rectangle that
815 connects both PCA graphs shows the Procrustes correlation quantifying the matching of soil
816 variables and species projections between the two PCAs ($P \leq 0.001$; MSR test). The histograms
817 show the relative eigenvalues of each PCA axis (only the first axis in each PCA expressed more
818 variation than expected under a broken stick model). Symbols in the graphs indicate whether
819 species are significantly indicative of one of the three habitats (seasonally flooded, terra firme,
820 or white-sand specialist) or not (generalist). Tables at the bottom show the Pearson correlations
821 of niche breadth (c) and niche position (d) values among soil variables. The significant
822 correlations (t -test of Pearson's moment correlation) are indicated in blue (grey values were not
823 significant).

824 **Figure 4.** Niche breadth–niche position relationship among the 246 species, for each of four
825 soil nutrients. Values indicated along x and y axes corresponded to back-transformed niche
826 breadth and niche position values, respectively. Traits significantly explained niche breadth
827 variation for N, Ca, and P. For these three nutrients, the Venn diagram on the right of the niche
828 breadth-position graph shows the relative linear contribution (adjusted R^2 from a variation
829 partitioning analysis) of niche position alone, traits alone, and the joint influence of niche

830 position and traits. Individual traits that significantly explained niche breadth variation (i.e., the
831 traits selected from a forward selection procedure, which was performed if the overall effect of
832 traits was significant when using the MSR testing procedure; see methods for details) were
833 indicated on the right of the Venn diagram, with colors indicating whether correlations were
834 positive (blue) or negative (red) between niche breadth and the trait. Symbols indicate whether
835 species are significantly indicative (significant indval) of one of the three habitats (see the
836 legend panel at the bottom right of the figure). The two grey regions in each graph represent
837 two different 95% Bayesian plausible intervals for predicted niche breadth values. The narrow
838 interval shows the distribution of estimated mean niche breadth values, while the wide interval
839 corresponds to the region in which the non-linear model expects to find 95% of actual niche
840 breadth values at each niche position value. The equation in each graph shows the median of
841 the Bayesian credibility interval for the linear and quadratic coefficients and the intercept.
842 Significant coefficients (i.e., at least 95% of estimated posterior coefficient values being
843 positive) were emphasized in bold. No significant quadratic effects were found for traits.
844 Asterisks in the Venn diagrams indicate significant adjusted R^2 values quantifying the relative
845 effect of niche position alone, traits alone and the co-variation of both niche position and traits,
846 according to the MSR testing procedure (see methods): *** $P \leq 0.001$; ** $P \leq 0.01$; * $P \leq 0.05$.
847





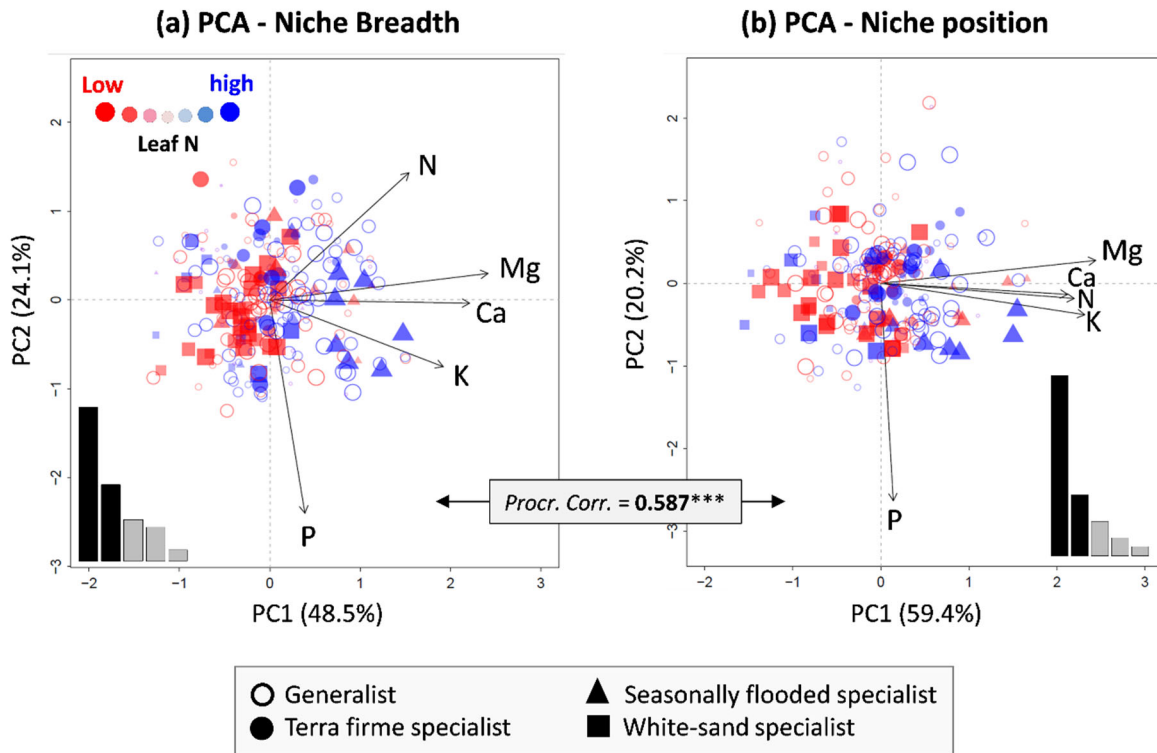
855

856 **Figure 2.**

857

858

859



(c) Niche breath correlations

	N	Ca	Mg	K
Ca	0.34			
Mg	0.45	0.77		
K	0.27	0.38	0.55	
P	-0.20	0.12	-0.01	0.23

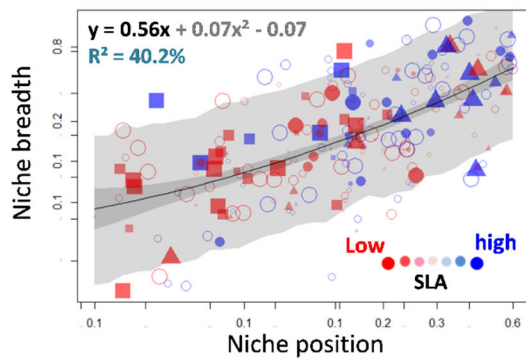
(d) Niche position correlations

	N	Ca	Mg	K
Ca	0.50			
Mg	0.64	0.74		
K	0.72	0.54	0.75	
P	0.09	0.11	-0.03	0.17

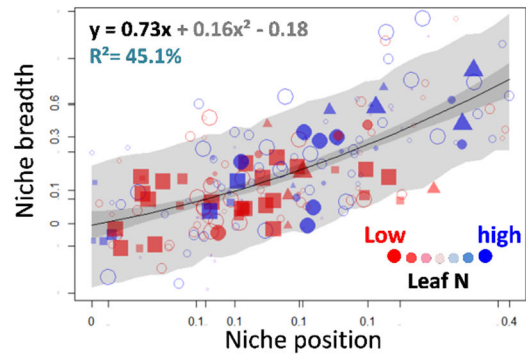
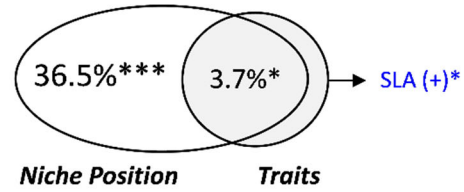
860

861 **Figure 3.**

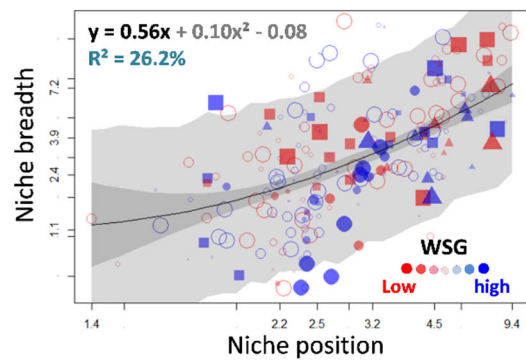
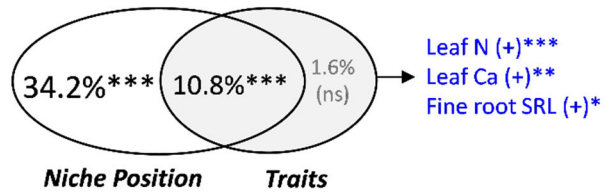
862



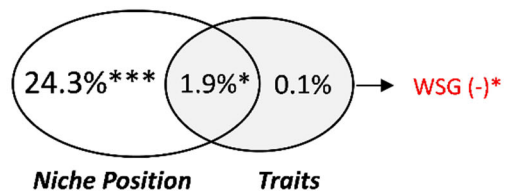
Soil N content



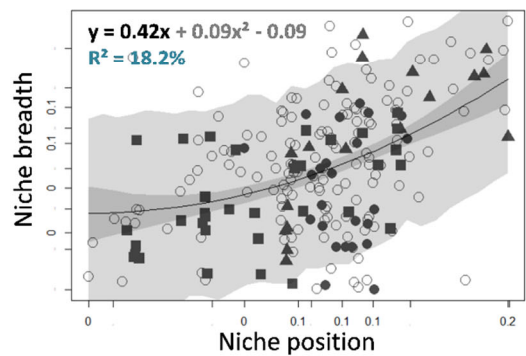
Soil Ca content



Soil P content



Soil K content



- Generalist
- ▲ Seasonally flooded specialist
- Terra firme specialist
- White-sand specialist

863

864 **Figure 4.**

865

866